Image Source Separation using Color Channel Dependencies *

Koray Kayabol[1]**, Ercan E. Kuruoglu[1], and Bulent Sankur[2]

[1] ISTI, CNR, via G. Moruzzi 1, 56124, Pisa, Italy,
koray.kayabol@isti.cnr.it, ercan.kuruoglu@isti.cnr.it,
[2] Bogazici University, Bebek, 80815, Istanbul, Turkey
bulent.sankur@boun.edu.tr

Abstract. We investigate the problem of source separation in images in the Bayesian framework using the color channel dependencies. As a case in point we consider the source separation of color images which have dependence between its components. A Markov Random Field (MRF) is used for modeling of the inter and intra-source local correlations. We resort to Gibbs sampling algorithm for obtaining the MAP estimate of the sources since non-Gaussian priors are adopted. We test the performance of the proposed method both on synthetic color texture mixtures and a realistic color scene captured with a spurious reflection.

1 Introduction

The problem of blind image separation is encountered in various applications such as document image restoration, astrophysical component separation, analysis of functional MRI (Magnetic Resonance Imaging) and removal of spurious reflections. Most of the previous studies for image source separation have assumed that the source signals are statistically independent. There are cases, however, where this assumption does not hold anymore. For example, the RGB components of a color image are known to be strongly correlated. We conjecture that a source separation algorithm that explicitly takes into consideration this prior information can perform better.

In this paper, we propose a Bayesian approach for the image source separation problem which takes the color channel dependencies into consideration using coupled MRF model. We limit our study to the separation of color image components, which are dependent, and an independent reflection source. The more general problem of source separation from multi-band observations, with interdependencies between the bands, is out of scope of this study. The application scenario is a color image corrupted by spurious reflections. Notice that reflection removal problem was addressed in [1] where at least two observed

* This project was supported by CNR-TUBITAK joint project No. 104E101.
** The research of Koray Kayabol at ISTI-CNR, Pisa, Italy is partially supported by ICTP, Programme for Training and Research in Italian Laboratories.

images were required. These had to be obtained in different lighting or under different polarization conditions [1]. In contrast our method can remove reflections by using only one observed color image.

The Bayesian frameset allows for under-determined linear mixture models, where the number of observations is smaller than the number of sources. For example, consider a color scene behind a transparent surface photographed with camera, but with an undesired achromatic reflection on the surface. We assume that reflected images are generally achromatic. In this case, the number of sources is four, with three dependent (RGB) components and the fourth one, the reflection, independent from them. Notice that the RGB components are considered as the three sub-sources of a single color source, which is itself mixed with an achromatic image. Since the source separation works with a single observed mixture image, the problem is severely under-determined. However, this under-determined problem is converted into a better posed one, by supplying the missing information via a constrained coupled MRF source model.

There are some recent papers that address the dependent source separation problem. For astrophysical images, Bedini et al. [2] proposed a method for correlated component separation, and Caiafa et al. [3] developed a technique for non-independent components using entropic measures. Gencaga et al. [4] proposed a method for separation of non-stationary mixtures of dependent sources. Hyvarinen and Hurri [5] and Kawanabe and Muller [6] developed separation methods for sources that have variance dependencies. There are also studies which investigate the frequency domain [7] and time-frequency [8] dependencies. Except for [2] and [3], these methods are all developed for dependent 1D signal separation applications.

We overcome the difficulty of separation of such under-determined and sparse models by using spatio-chromatic coupled MRF source models. The coupled MRF model takes both the inter- and the intra-channel dependencies into account. To obtain the MAP estimate of the sources we used Gibbs sampling [9], which is a fully Bayesian algorithm. The algorithm used in this study is an extension of the algorithm in [10].

2 Problem Definition in the Bayesian Framework

In this study, we limit our study to the mixture case of a trichromatic color image and an achromatic component, which results in a single observed color image. The three components of the observed image are $y_j(n), j \in \{r, g, b\}$, where n indexes the pixels. Thus in the parlance of source signal separation one has $L = 4$ sources, $s_i(n)$, $i \in \{r, g, b, m\}$ and $K = 3$, $y_j(n), j \in \{r, g, b\}$ observations. The linear mixing model is given as:

$$\begin{bmatrix} y_r(n) \\ y_g(n) \\ y_b(n) \end{bmatrix} = \begin{bmatrix} a_{r,r} & 0 & 0 & a_{r,m} \\ 0 & a_{g,g} & 0 & a_{g,m} \\ 0 & 0 & a_{b,b} & a_{b,m} \end{bmatrix} \begin{bmatrix} s_r(n) \\ s_g(n) \\ s_b(n) \\ s_m(n) \end{bmatrix} + V \tag{1}$$

where V is a zero-mean Gaussian noise vector with $\Sigma = \text{diag}\{\sigma_r^2, \sigma_g^2, \sigma_b^2\}$ covariance matrix. Noise terms are independent identically distributed (iid) in every pixel of the three component images.

When we formulate the BSS problem in the Bayesian framework, the joint posterior density of unknowns $\mathbf{s}$ and $\mathbf{A}$ can be written as:

$$p(\mathbf{s}_{r,g,b,m}, \mathbf{A}|\mathbf{y}_{r,g,b}) \propto p(\mathbf{y}_{r,g,b}|\mathbf{s}_{r,g,b,m}, \mathbf{A})p(\mathbf{s}_{r,g,b,m}, \mathbf{A}) \tag{2}$$

where $\mathbf{s}$ and $\mathbf{y}$ are lexicographically ordered vector representation of source and observation images, respectively. The unknown sources and the elements of the mixing matrix must be found by using their joint posterior density in (2).

Since the joint solution of (2) is not tractable, we must separate the problem into more manageable parts. According to the source and observation models, we assume that the mixing matrix and the sources are mutually independent, and also the achromatic source is independent from the color image. But the components of the color image are dependent. Using the Bayes rule, conditional densities for sources and mixing matrix can be written as:

$$p(\mathbf{s}_{r,g,b}|\mathbf{s}_m, \mathbf{y}_{r,g,b}, \mathbf{A}) \propto p(\mathbf{y}_{r,g,b}|\mathbf{s}_{r,g,b,m}, \mathbf{A})p(\mathbf{s}_{r,g,b}) \tag{3}$$

$$p(\mathbf{s}_m|\mathbf{s}_{r,g,b}, \mathbf{y}_{r,g,b}, \mathbf{A}) \propto p(\mathbf{y}_{r,g,b}|\mathbf{s}_{r,g,b,m}, \mathbf{A})p(\mathbf{s}_m) \tag{4}$$

$$p(\mathbf{A}|\mathbf{s}_{r,g,b,m}, \mathbf{y}_{r,g,b}) \propto p(\mathbf{y}_{r,g,b}|\mathbf{s}_{r,g,b,m}, \mathbf{A})p(\mathbf{A}) \tag{5}$$

One can use the maximum-a-posteriori (MAP) estimate by alternating variable approach, such as Iterated Conditional Mode. Difficulties may arise in MAP estimation due to non-Gaussian prior densities since they disturb the convexity of the MAP estimate. So we resort to Markov Chain Monte Carlo-based (MCMC) numerical Bayesian methods such as Gibbs sampling.

We use Gibbs sampler to break down the multivariate sampling problem into a set of univariate ones [9]. This iterative procedure continues until the samples converge to those that would have been obtained by sampling the joint density. Our random sampling scheme from source images is hybrid wherever we cannot use direct sampling methods, in other words Metropolis steps are embedded within Gibbs sampling. The normalization term of the Gibbs distribution, namely the partition function, is intractable. Since the posterior of a pixel is formed by the product of a Gaussian likelihood and a Gibbs prior, the posterior is also intractable and direct sampling is not possible. Therefore we resort to Metropolis steps.

After sampling all the images with Metropolis method, the next step is drawing samples from the mixing matrix. When all of the unknowns are sampled, one iteration of the Gibbs sampling algorithm is completed. The Gibbs sampling modified by embedded Metropolis steps, as used in this study, is given in Table 1.

for all source image, $l = r, g, b, m$

for all pixels, $n = 1 : N$
Using Metropolis method
$s_l^{t+1}(n) \longleftarrow \text{sample}_{s_l(n)} \left\{ p(s_l(n) | \mathbf{s}_{l\backslash(n)}^t, \mathbf{s}_{\{r,g,b,m\}\backslash l}^t, \mathbf{y}_{r,g,b}, \mathbf{A}^t) \right\}$

for all elements of mixing matrix, $(k, l) = (1, 1) : (K, L)$

$a_{k,l}^{t+1} \longleftarrow \text{sample}_{a_{k,l}} \left\{ p(a_{k,l} | \mathbf{A}_{-(k,l)}^t, \mathbf{y}_{r,g,b}, \mathbf{s}_{r,g,b,m}^t) \right\}$

Table 1. Gibbs sampling algorithm.

3 Observation Model

Since the observation noise is assumed to be iid zero-mean Gaussian at each pixel, the likelihood is also Gaussian such that

$$p(\mathbf{y}_{r,g,b} | \mathbf{s}_{r,g,b,m}, \mathbf{A}) = \prod_{k \in \{r,g,b\}} \mathcal{N}(\mathbf{y}_k | \bar{\mathbf{y}}_k, \sigma_k^2) \tag{6}$$

where $\mathcal{N}(\mathbf{y}_k | \bar{\mathbf{y}}_k, \sigma_k^2)$ represents a Gaussian density with mean $\bar{\mathbf{y}}_k$ and variance σ_k^2 and

$$\bar{\mathbf{y}}_k = \sum_{l=1}^{L} a_{k,l} \mathbf{s}_l, \qquad L = 4. \tag{7}$$

The prior distributions of elements of $\mathbf{A}$ are chosen as a non-negative uniform distribution due to the lack of any information to the contrary.

$p(a_{k,l}) = [u(a_{k,l}) - u(a_{k,l} - A_{max})]/A_{max}$ where A_{max} is the maximum allowable value of the mixing matrix and $u(.)$ is the unit step function. Using this prior and likelihood in (6), the posterior density of $a_{k,l}$ is formed as

$$p(a_{k,l} | \mathbf{y}_{r,g,b}, \mathbf{s}_{r,g,b,m}, \mathbf{A}_{-a_{k,l}}, \sigma_{1:K}^2) \propto \mathcal{N}(a_{k,l} | \mu_{k,l}, \gamma_{k,l})[u(a_{k,l}) - u(a_{k,l} - A_{max})]. \tag{8}$$

The mean $\mu_{k,l}$ and the variance σ_k^2 are calculated only for the nonzero elements of the mixing matrix in (1) such that

$$\mu_{k,l} = \frac{1}{\mathbf{s}_l^T \mathbf{s}_l} \mathbf{s}_l^T (\mathbf{y}_k - \sum_{i \in \{r,g,b,m\}, i \neq l} a_{k,i} \mathbf{s}_i) \tag{9}$$

and $\gamma_{k,l} = \sigma_k^2 / \mathbf{s}_l^T \mathbf{s}_l$ and $l \in \{r, g, b, m\}$ and $k \in \{r, g, b\}$.

4 Source Model

Two source models have been used in this study; one of them is for achromatic source and the other is for the color source.

4.1 Achromatic Source Model

For independent achromatic source, we assume that it is modelled as MRFs and that its density $p(\mathbf{s}_m)$ is chosen as Gibbs distribution with possibly non-convex energy potential function. The energy function of Gibbs distribution is

$$U(\mathbf{s}_m) = \frac{1}{2} \sum_{\{n,q\} \in \mathcal{C}} \beta_m \rho_m (s_m(n) - s_m(q)) \tag{10}$$

where $\rho_m(.)$ is the non-convex potential function and $\mathcal{C}$ is the entire clique set. The Gibbs distribution is given as

$$p(\mathbf{s}_m) = \frac{1}{Z(\beta_m)} e^{-U(\mathbf{s}_m)} \tag{11}$$

where $Z(\beta_m)$ and β_m are the partition function and the parameter of MRF, respectively.

In this work we opt to describe pixel differences in terms of iid Cauchy density. Notice that while pixels are dependent, the pixel differences can often be modeled as an iid process [10]. Then the clique potential of the Gibbs density under Cauchy assumption becomes:

$$\rho_m(s_m(n) - s_m(q)) = \ln \left[1 + \frac{(s_m(n) - s_m(q)))^2}{\delta_m} \right] \tag{12}$$

where δ_m is the scale parameter of Cauchy distribution and is called also as threshold parameter of the regularization function. In this study, both of the β_m and δ_m parameters are assumed homogeneous over the MRF.

4.2 Color Source Model

For the prior of the color image, we use multivariate Cauchy density. The clique potential of dependent color component $\mathbf{s}_c(n) = [s_r(n) \quad s_g(n) \quad s_b(n)]^T$ can be written as

$$\rho_c(\mathbf{s}_c(n) - \mathbf{s}_c(q)) = \frac{5}{2} \ln \left[1 + [\mathbf{s}_c(n) - \mathbf{s}_c(q)]^T \Delta^{-1} [\mathbf{s}_c(n) - \mathbf{s}_c(q)] \right]. \tag{13}$$

where Δ is 3×3 symmetric matrix which defines the correlation between color channels. Again we want to point out that these correlations are between pixel differences, which implies that the component edge images are mutually correlated. Our model does not assume any correlation between the pixel values directly, so that $\rho_c(.)$ is a function of pixel differences $[\mathbf{s}_c(n) - \mathbf{s}_c(q)]$. only. The choice of a non-convex clique potential function helps to preserve the edges. The matrix Δ can be expressed explicitly as

$$\Delta = \begin{bmatrix} \delta_{r,r} & \delta_{r,g} & \delta_{r,b} \\ \delta_{r,g} & \delta_{g,g} & \delta_{g,b} \\ \delta_{r,b} & \delta_{g,b} & \delta_{b,b} \end{bmatrix} \tag{14}$$

and the elements of this matrix are defined by the user.

Table 2. PSIR (dB) results of the separated sources under dependence and independence assumptions. While source 1 has red, green and blue components, source image 2 consists of only one gray-valued component.

	red	green	blue	achromatic
Dependence assumption	48.98	37.69	36.39	38.55
Independence assumption	48.30	31.83	25.75	34.76

5 Simulation Results

We illustrate the performance of the proposed dependent color source separation algorithm with two examples: The first example consists of a synthetic mixture of texture images, while the second one is real mixture case actually taken with a camera. We use the Peak Signal-to-Inference Ratio (PSIR) as performance indicator. Furthermore, we assume that the correlation coefficients of the color components in (14) as well as the variances of the noise terms in (1) are known or user defined.

5.1 Synthetic Mixture Case

The mixture consists of a color texture image whose components are dependent and another gray-valued texture image independent of the color image. Sample images of original textures and their mixtures are shown in the first and second columns of Fig. 1, respectively. The true color version of the original color image and mixtures (observation) can be seen in Fig. 2. The mixing matrix was chosen as

$$\mathbf{A} = \begin{bmatrix} 1.0 & 0 & 0 & 0.4 \\ 0 & 0.7 & 0 & 0.6 \\ 0 & 0 & 0.5 & 0.8 \end{bmatrix}. \tag{15}$$

These results are compared with those obtained under independent color channels assumption. The PSIR (dB) results obtained under dependence and independence assumptions are shown in Table 2. To obtain the results for the independence assumption, the source model and the algorithm in [10] was used. Dependence assumption yields better results as compared to the independence assumption. For example, the blue component is not separated under independence assumption.

5.2 Real Mixture Case

For a realistic application, we used a color image taken with digital camera and corrupted by a reflection as in Fig. 3 (a)[3]. The scene is organized such that a toy is standing behind a transparent CD box and a reflection occurs on the box

[3] The authors would like to thank to Alpay Kucuk for taking the photograph used in Sect. 5.2.

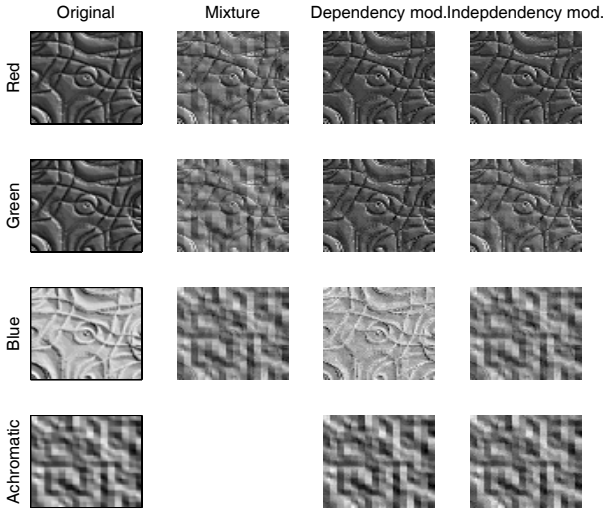

Fig. 1. Simulation experiments with noiseless texture images. First column: original images; second column: images mixed with $\mathbf{A}$ in (15); third column: sources estimated with dependence assumption; fourth column: sources estimated with independence assumption.

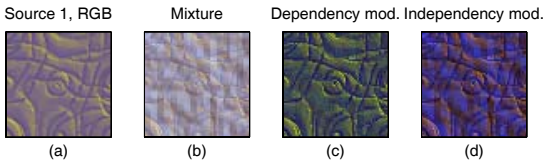

Fig. 2. True color images: (a) original color texture, (b) true color mixture (observation), (c) and (d) estimated color texture under dependence and independence assumption, respectively.

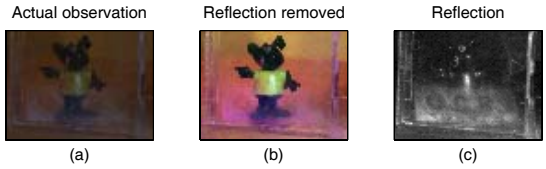

Fig. 3. Removal of reflection image mixed to a color image. (a) Observed actual mixed image, (b) Color image with mixed reflection removed , (c) Estimated achromatic reflection image.

surface. The reflection is assumed as an achromatic source while the scene behind is a color image source. We were justified in using the proposed linear mixing model in (1) since the reflection image is both transparent and additive. However, as would occur in real-life situations, the mixing is not stationary, which means that the mixing matrix changes from pixel-to-pixel. Although the mixing is not stationary since the amount of reflection has been changing over the surface, the separation results are quite satisfactory as shown in Fig. 3 (b) and (c). The entries of the Δ matrix has been manually tuned to optimal values by trial and error. The color image of the toy scene is well separated with the reflection almost removed while the achromatic reflection component still contains some vestige of the color image.

6 Conclusion

In this study, we have proposed statistical models for blind separation of dependent source images, and have shown that taking into account the prior information on the dependence of color components results in higher performance as compared to the independence model. The proposed model can find application in color document analysis, restoration of ancient documents and polarized image applications. In a follow-up study we will extend the algorithm for automatic estimation of MRF parameters and noise variances.

References

1. Bronstein, A. M., Bronstein, M. M., Zibulevsky, M., Zeevi, Y. Y.: Sparse ICA for blind separation of transmitted and reflected images. Int. J. Imaging Science Technology, 15, 84–91, (2005)
2. Bedini, L., Herranz, D., Salerno, E., Baccigalupi, C., Kuruoglu, E. E., Tonazzini, A.: Separation of correlated astrophysical sources using multiple-lag data covariance matrices, EUROSIP Journal on Applied Signal Processing, 15, 2400–2412, (2005)
3. Caiafa, C. F., Kuruoglu, E. E., Proto, A., N.: A minimax entropy method for blind separation of dependent components in astrophysical images. AIP-Proceedings of MaxEnt 2006, 81–88, (2006)
4. Gencaga, D., Kuruoglu, E. E., Ertuzun, A.: Bayesian separation of non-stationary mixtures of dependent Gaussian sources. AIP-Proceedings of MaxEnt 2005, (2005)
5. Hyvarinen, A., Hurri, J.: Blind separation of sources that have spatiotemporal variance dependenies. Signal Process., 84, 247–254, (2004)
6. Kawanabe, M., Muller, K.-R.: Estimating functions for blind separation when sources have variance dependenies. Journal Machine Learning, 6, 453–482, (2005)
7. Zhang, K., Chan, L.-W.,: An adaptive method for subband decomposition ICA. Neural Computation, 18, 191–223, (2006)
8. Abrard, F., Deville, Y.: A time-frequency blind signal separation method applicable to underdetermined mixtures of dependent sources. Signal Process., 85, 1389–1403, (2005)
9. Gilks, W. R., Richardson, S., and Spiegalhalter, D. J.: Markov Chain Monte Carlo in Practice, London, U.K.: Chapman & Hall, (1996)
10. Kayabol, K., Kuruoglu, E. E., Sankur, B.: Bayesian separation of images modelled with MRFs using MCMC. IEEE Trans. Image Process., (accepted), (2008)